Research Report

Segmentation and Estimation of Lung Structures for Ventilation and Perfusion Analysis

Author:
Johannes Hofmanninger
j.hofmanninger@gmail.com

February 28, 2013

Acknowledgements

First of all, I would like to express my deepest gratitude to Prof. Dr. Reinhard Beichel and Dr. Christian Bauer for supervising my work, patience guidance and pleasant collaboration. For sharing your professional expertise and giving me an unique opportunity to learn and improve.

I would like to thank Dr. Robb W. Glenny and Dr. Melissa A. Krueger from the Division of Pulmonary & Critical Care Medicine at the University of Washington for providing image data and helpful feedback.

I am especially thankful to the Austrian Marshall Plan Foundation who made this work possible in the first place and giving me this unique opportunity.

Abstract

In this work, methods for the segmentation of lung structures in multi-spectral cryomicrotome images of rat lungs are developed and investigated. Specifically, different approaches to segment/estimate supply regions of airway subtrees are presented. In addition, functional units of the lung are segmented utilizing ventilation images. The presented work facilitates the calculation of local ventilation and perfusion ratios and allows researchers to put these ratios in relation to airway and lung vessel geometries, which represents a valuable tool for studying normal and diseased lungs.

Contents

1 Background & Introduction

The ratio of Ventilation to Perfusion in lungs is a measurement to assess the efficiency of gas exchange. Only if regional ventilation and blood flow are closely matched, gas exchange can take place efficiently. A detailed understanding of these mechanisms can help to develop more effective treatments for lung diseases like chronic obstructive pulmonary disease (COPD), emphysema, acute lung injury, or bronchopulmonary dysplasia. The team of Professor Dr. Robb W. Glenny from the Division of Pulmonary & Critical Care Medicine at the University of Washington are utilizing cryomicrotome imaging of rat lungs to provide high-resolution information about lung anatomy and maps of regional ventilation and perfusion. This multispectral rat lung image data facilitates analysis of the relation between regional perfusion, ventilation, as well as airway and vascular tree geometries.

The objective of this work is to segment and estimate lung structures to allow the study of perfusion and ventilation in regional lung areas. The partitioning of the lung into lobes, sub-lobes and even smaller functional compartments will allow to analyse the above mentioned relationships.

Depending on the local region size of interest and the utilized cryomicrotome image channel, different algorithms have been developed to segment such regions. Furthermore, computer-aided methods have been developed to generate perfusion and ventilation measurements for these regions.

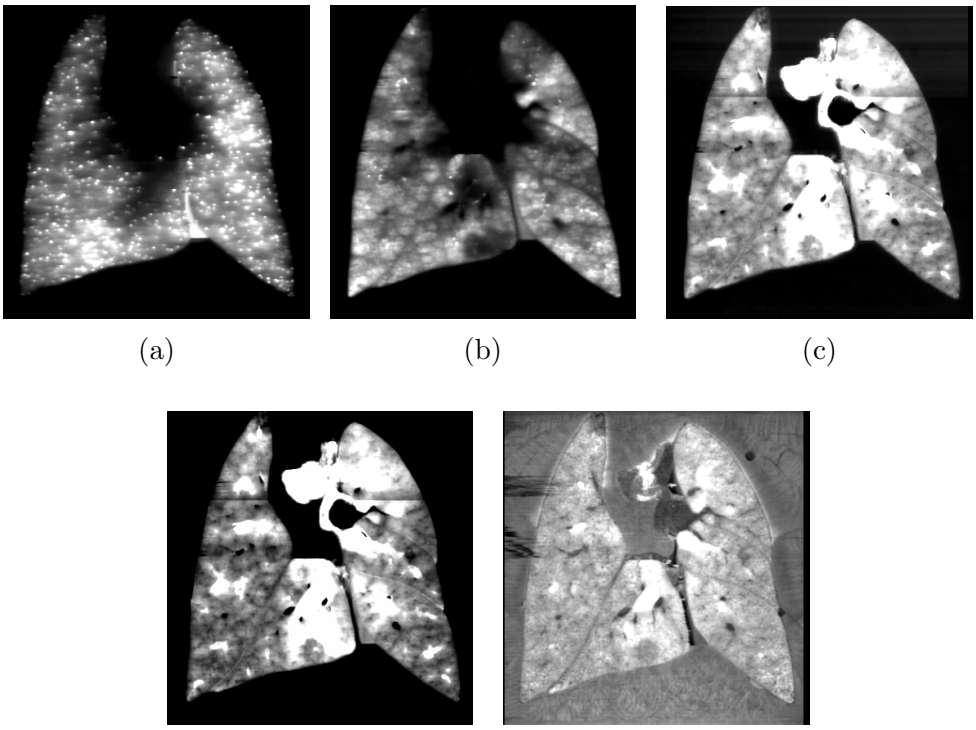

(a) (b) (c)

(d) (e)

Figure 1: Image channels. (a) Scarlet channel (sc-channel), depicting the microspheres used to estimate blood flow. (b) Red channel (rd-channel), shows the aerosol distribution for ventilation estimation. (c) and (d) Fluorescent channels (fl- and f2-channel), emphasizes airways and vessel walls. (e) Outline channel (ol-channel), highlights the lung parenchyma and vessel lumen.

2 Data

2.1 Imaging

The Imaging CryoMicrotome (Barlow Scientific, Inc. Olympia WA) was developed in collaboration with Dr. Glenny at the University of Washington and is a device that determines the spatial distribution of fluorescent microspheres in an organ at the microscopic level and obtains transverse images of the organ. The instrument is housed in Dr. Glenny's laboratory at the Uni-

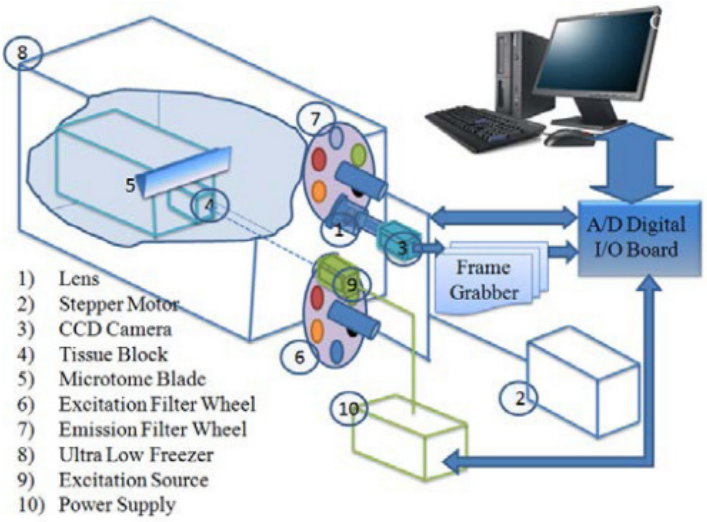

Figure 2: The imaging cryomicrotome. Image by [1]

versity of Washington and consists of a Redlake MegaPlus II ES 3200 digital camera (Redlake, San Diego, CA) with a resolution of 2,184×1,472 pixels, a computer (Dell Computer Corp., Round Rock, Texas), metal halide lamp (HTI 403W/24, Osram, Sylvania), excitation filter-changer wheel, emission filter-changer wheel, and a cryostatic-microtome. Fluorescence images are acquired with the Redlake digital camera with a 200 mm Nikkor lens (Nikon, Corp., Tokyo, Japan). Two motorized filter wheels containing excitation and emission filters are controlled by the computer through stepper motors and microsensors (Fig. 2). The cryomicrotome serially sections through the frozen organ with a slice thickness of $25\mu m$ while maintaining the sample in a rigid x and y position to assure precise alignment of serial images. Digital images of the remaining tissue surface are acquired with appropriate excitation and emission filters to isolate each fluorescent color and to obtain grey-scale images of the organ surface (Fig. 1). The spatial resolution of the system depends on the magnification used to image the organ, but is

typically 25 μm in the X/Y and also 25μm in the Z direction.

Sprague-Dawley rats weighting approx. 250g got anesthetized by intraperitoneal injections of 140-160mg/kg pentobarbital, sufficient to prevent withdrawal of paw after pinch. A tracheostomy was performed, and an internal jugular vein cannulated. The animals were mechanically ventilated at a rate of 40breaths/min with a tidal volume of 4 ml, utilizing a piston pump ventilator. A fluorescent microsphere aerosol was generated by an inline ultrasonic aerosol-generating system (Microstat Ultrasonic Nebulizer, Mountain Medical Equipment, Littleton, CO) that passes the generated aerosol through 2 drying columns before entry into the trachea. The fluorescent microsphere aerosol was generated from 2ml of a 2.5% suspension of 0.04μm FMS (Molecular Probes, Eugene, OR) in distilled water and administered to the rats for 5 min. Regional blood flow to rat lungs was marked by intravenous injection of 40,000 FMS (15μm) of a different color. Each rat was then deeply anesthetized with 100mg/kg ip pentobarbital and exsanguinated. The lungs were cut free from cardiac and mediastinal tissues. The pulmonary artery was cannulated and the pulmonary vasculature filled with 96% OCT (optimal cutting temperature media, Tissue-Tek OCT) and 4% India ink until the left atrium was well filled. The lungs were filled via tracheal injection of 6 to 8 ml of 100% OCT. The filled lungs were frozen, suspended in a mixture of 90% OCT and 10% India ink, and frozen in the suspension OCT mixture. The frozen tissue block was fixed in the cryomicrotome and shaved with 16μm increments. Images of the enface block were captured with white light and with appropriate combinations of excitation and emission filters, resulting in different spectral channels. Each

transverse plane was imaged with specific band-pass filter pairs that highlighted specific structures (Fig. 1). A rat lung requires 2500-3000 16 μm thick slices to image the entire lung. Each image is 2184×1472 pixels and results in a file size of approx. 1-1.5MB (loss-less compression). With a minimum of 4 images per slice, each rat lung requires approximately 18GB of storage. Hence one of the significant challenge of this work was to develop algorithms that efficiently handle these large data sets. All cross-sectional image sets were converted to volumetric data sets to facilitate the 3d segmentation of anatomical structures like lobes and airway supply regions. In this study, 5 cryomicrotome data sets were utilized.

2.2 Data preprocessing

The spatial location of every fluorescent microsphere representing blood flow and information about ventilation (aerosol distribution) at each voxel was provided for all data sets. The locations have been determined by a software developed by Dr. Glenny's laboratory at the University of Washington.

The segmentation of the airways was done by Dr. Beichel's Lab with methods adapted for Cryomicrotome images. The airways were made available not only as a mask volume, but also as a tree structure derived from the centerline representation.

Besides the image data sets and the microsphere locations, a segmentation of high gray-value (lung) areas in the volumes based on thresholding was provided. This mask separated the background from lung voxels (Fig. 3a and 3b).

Based on such masks, the lobe and lung masks were created using an

already developed plug-in tool for 3DSlicer[1].

The first step was to break down the lung to its well defined substructures, the lobes. The segmentation of the five lung lobes was accomplished with a semiautomatic technique to split down the provided volume masks. To divide the masks, the tissue called fissures which separates the lobes was manually marked by fiducials in a sufficient number of cross-sections (Fig. 3b). The slicer tool then separated the mask by creating a b-spline surface on basis of the manually set fiducials (Fig. 3c). Through recursive application of this technique on the gained splitted masks, the lobes were separated and tissue not belonging to the lung like heart tissue or trachea was excluded with the same procedure.

Figure 3d shows a lung with its five segmented lobes. All further processing steps to estimate compartments were applied on each individual lobe. Motivated by lung anatomy, this ensures that every compartment belongs to a certain lobe without the risk of wrong assignments among lobes and therefore distortion in the resulting data. The final lung mask was created by merging the five lobe masks.

3 Supply Region Estimation

3.1 Introduction

To analyse and compare measurements like perfusion microsphere-counts, voxelwise approaches are not suitable, because the microspheres used for perfusion estimation are too sparsely distributed. To investigate a possible

[1] www.slicer.org

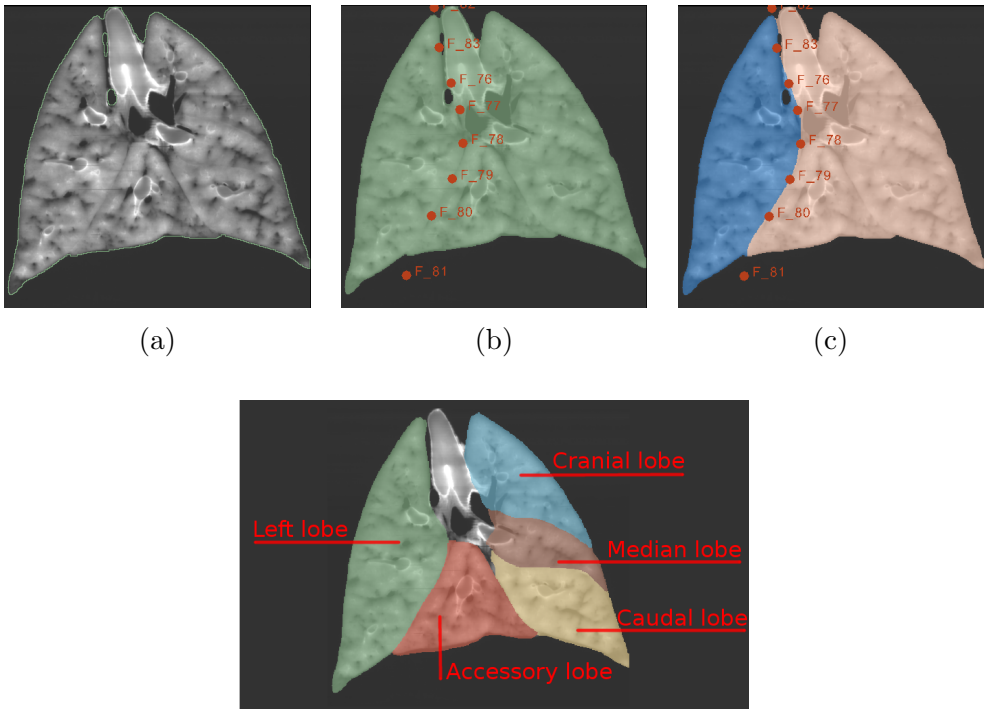

(a) (b) (c)

(d)

Figure 3: Lung lobe segmentation. (a) Threshold based tissue mask. (b) Manually set fiducials along a fissure. (c) B-spline surface dividing the masked area. (d) Segmented lobes. Note the excluded heart and trachea region.

correlation, local areas have to be chosen for this type of analysis. Furthermore, to study the correlation of geometric tree properties of the airway and blood vessels with perfusion and ventilation measures from the cryomicrotome images the size of supply areas of airway outlets or airway-subtrees have to be estimated.

Motivated by lung anatomy, different approaches have been developed and implemented to divide the lung into smaller regions to allow analyses on different levels. The lobes can be considered as the highest level of lung sub-structures in which gas exchange occurs. Every lobe of a lung is divided in so called secondary lobes. This sub-lobes are the areas of the

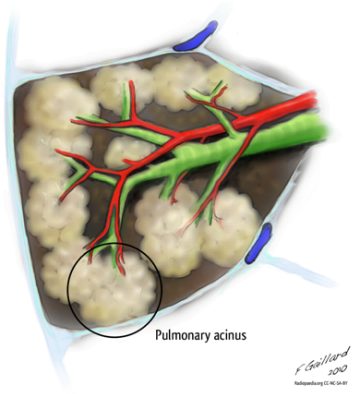

Figure 4: Lung acini. Schematic illustration of acini gathered in a secondary pulmonary lobe. *Image: Frank Gaillard, License: CC-NC-BY-SA*

lung supplied by the sub-trees of the main airway branch. The size of these Sub-lobes can be estimated based on the structure of the airway tree. This approach doesn't work at a smaller level of lung structures like the so called acini (Fig. 4) as the airways are too small at this level to get detected in the images. However, since acini regions are visible in the aerosol images, a bottom up approach to segment these compartments was developed.

3.2 Methods

The graph in Fig. 5 gives a rough overview of the basic processing steps to estimate the supply regions. The input data used are the aerosol images (rd-channel), the segmented airways and their skeleton. As mentioned above, the airway-segmentation and tree-generation from the centerlines was done by Dr. Beichel's laboratory with previously developed methods. The lung-lobe segmentation was performed with a semiautomatic method in 3DSlicer. All methods to segment the acini and estimate the supply regions of sub-trees and airway outlets have been implemented in C++ using the "Insight

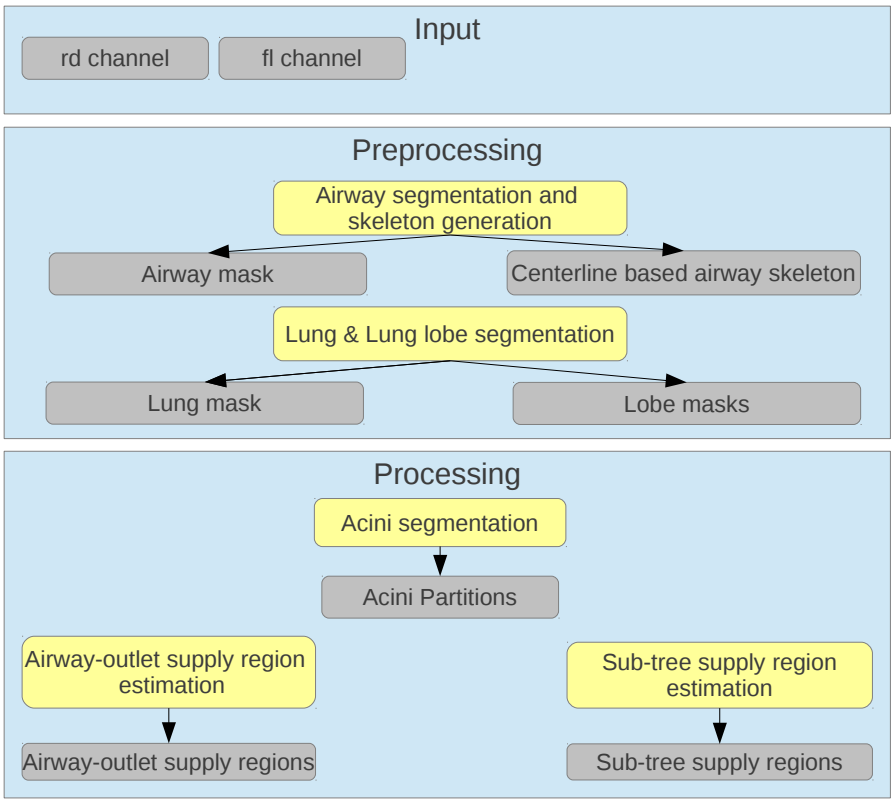

Figure 5: Processing pipeline overview. Input: rd- and fl-channel. Preprocessing: The airway segmentation and the lobe segmentation.

Segmentation and Registration Toolkit"(ITK)[2].

3.2.1 Acini Segmentation

The acini structures are assumed to appear in the rd-channel (aerosol images) as areas with higher gray values in a characteristic shape. A physician annotated some structures on a slice of an aerosol image to give some impression on size and shape (Fig. 7).

To segment these areas, a watershed transformation with suitable pre-

[2]www.itk.org

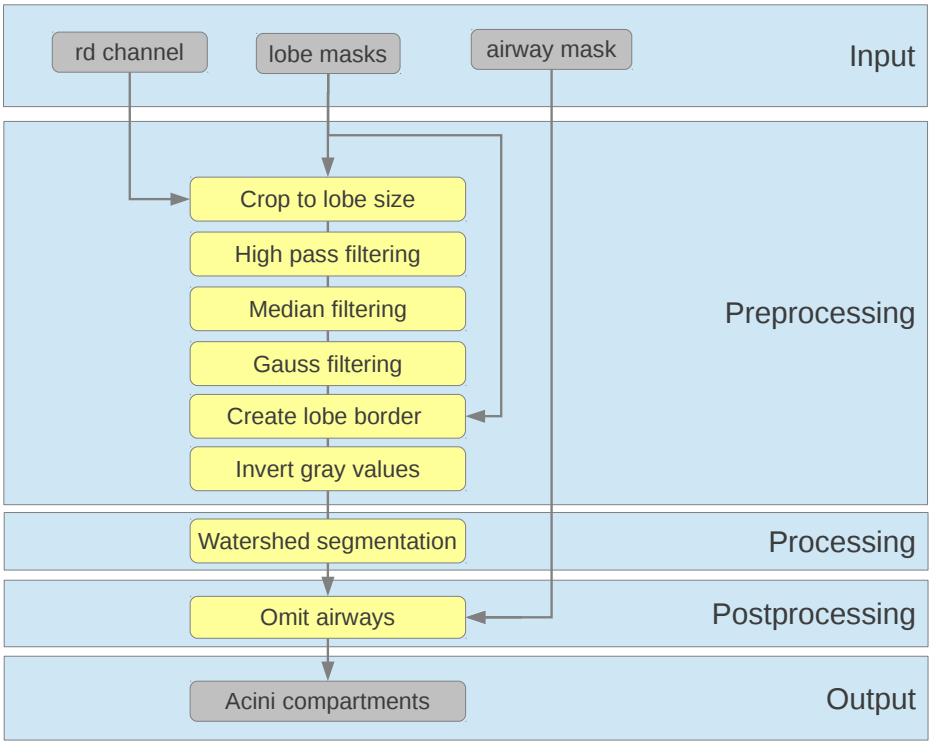

Figure 6: Processing Pipeline for segmenting acini.

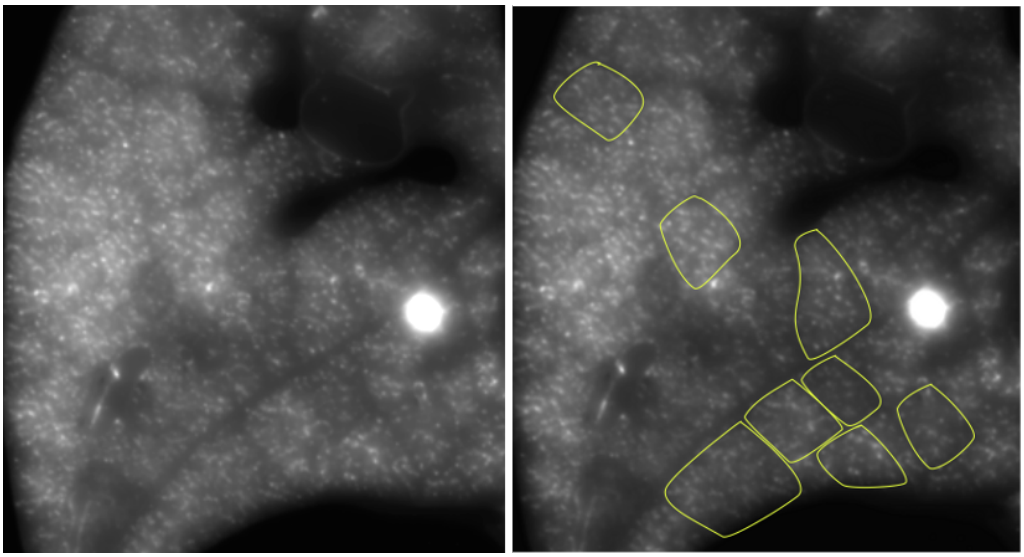

Figure 7: Acini structures annotated from a physician on an aerosol image.

and postprocessing was applied. An overview on methods and data used is given in Fig. 6, and a detailed description of individual processing steps is given below.

Preprocessing The prepossessing steps highly influence the performance of the watershed segmentation method, because the target structures have to be accentuated while disturbing image information has to be eliminated as good as possible to obviate over- and under-segmentation. For segmenting the acini, the channels fl and rd were considered. However, the rd channel was the most promising and some experiments to combine the two channels information didn't produce better results. So only the rd-channel information was used for segmenting the acini structures. The inhomogeneous gray value distributions within the structures visible in the rd-channel can lead to over segmentation when applying watershed. The low frequency gray value variations primarily cause under segmentation.

Preprocessing Steps:

Highpass filtering A high-pass filter was used to reduce the low frequency gray value variations within the lobes. Intensity differences covering multiple target structures could lead to over segmentation in the areas with high values and under segmentation in the low intensity areas, because the watershed transformation is using the maximum gray value in the volume as reference. The effect of the high-pass filter can be seen by comparing Fig. 8a to Fig. 8b.

Median filtering Median-filtering allowed to get rid of small high gray

value peaks as well as preserve the darker areas between the accumulations. The choice of kernel size was critical. When the size was chosen too big the compartments were not separated good enough which led to over segmentation. On the other hand, when the kernel size was chosen too small, high frequency gray-value variations lead to over-segmentation. The Size of 4x4x4 Voxel showed good results. Fig. 8c shows a volume after highpass filter and median filter were applied.

Gauss filtering A gauss filter was used to provide smoother transitions for the watershed (Fig. 8d). This was a further step to prevent over segmentation. A too strong smoothing however would lead to under-segmentation.

Creating a lobe border To ensure the watershed-segmentation will segment along the lobe border an artificial watershed was added. As the image gets inverted right before the watershed step (see next processing step), at this time the border consists of very low gray value pixel along the lobe exterior. The value should be significant lower than the image background values to produce a high enough gradient for the watershed.

Inverting the gray values The last preprocessing step was the gray-value inversion. As we want to get the high gray-value areas and the watershed is segmenting low gray-value basins, thus the volume was simply inverted. Figure 8e shows the inverted volume and the high-value border.

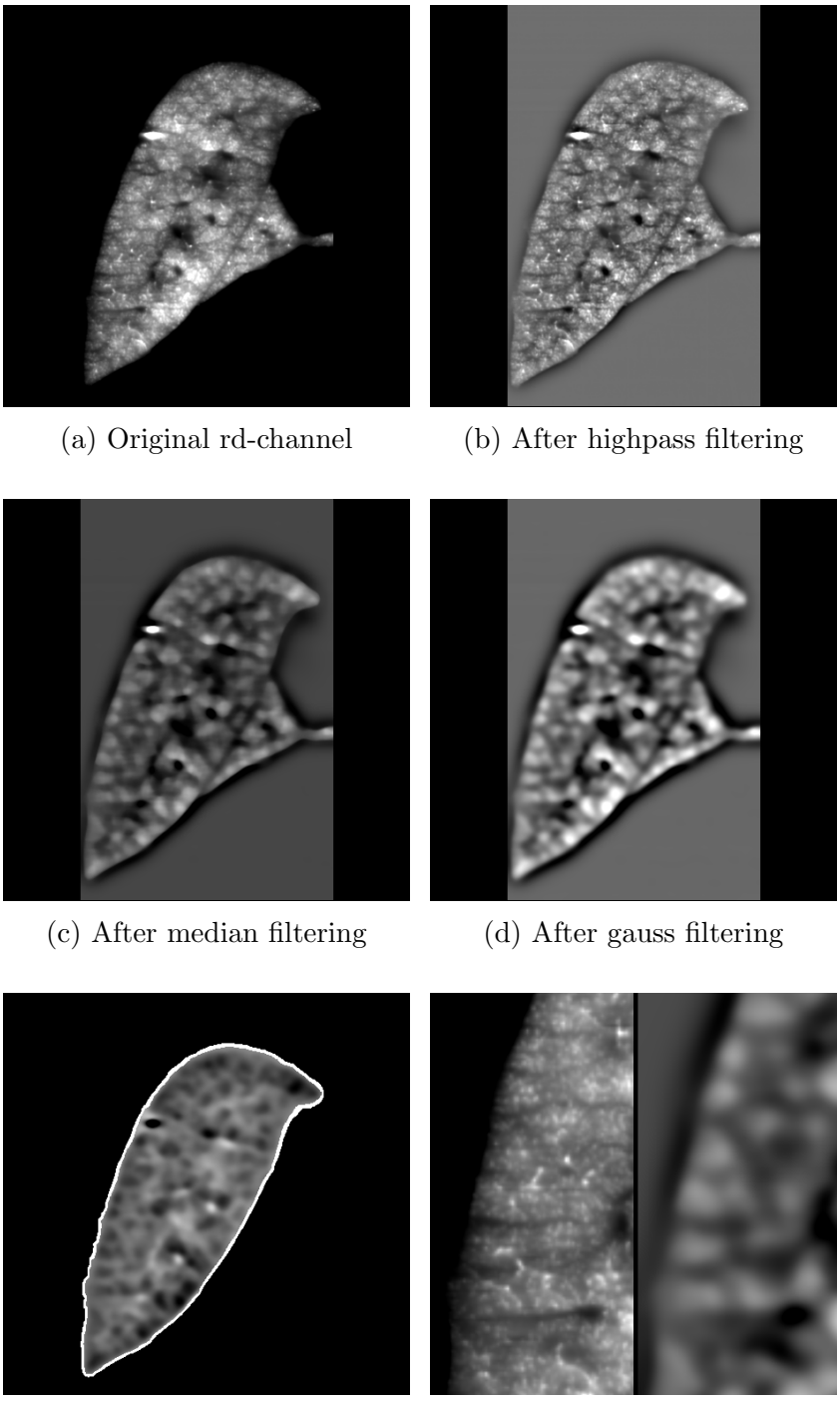

(a) Original rd-channel

(b) After highpass filtering

(c) After median filtering

(d) After gauss filtering

(e) Inverted and border created

(f) Left: original, Right: after gauss filtering

Figure 8: Preprocessing steps for Watershed segmetnation. Corss-section of a left-lobe showing the rd-channel volume after different preprocessing steps (see text).

Figure 8f shows a the differences between the original (Fig. 8a) and the finally smoothed volume (Fig. 8d).

Watershed transformation A grayscale image can be interpreted as a topographic relief, where each pixel represents the elevation at the pixels position. Considering this way on looking at scalar grayscale representations of data, Digabel and Lantuejoul proposed the watershed transfrom as an image processing tool in the early 90's.

The watershed segmentation is generated in several steps. An initial classification of all pixels into basin regions is done by tracing each point down its path of steepest descent to a local minima. In the next step precipitation that rains into the basins is simulated. Based on the "flood level", a value that reflects the amount of precipitation, adjacent basins are merged based on some saliency measure (like minimum boundary height). Considering the rising flood a merge tree can be retrieved. From top to down, this merge tree contains from just one big to many small segments.

The ITK implementation was used to perform the watershed transformation on the preprocessed images. To control the segmentation process, the "level parameter" is utilized. The level parameter influences the amount of segments created. He represents the "water-level" and corresponds to the difference between the lowest and highest gray value in the volume in percent. A lower level parameter produces more segments and an elevated level parameter decreases the number and generates bigger segments. Subjectively, a value of 5 showed the best results.

After the watershed was applied, the airways were omitted, because within them, there is no gas exchange occurring.

Results Figure 9b shows a cross-section of a watershed segmented left lobe with omitted airways. Figure 9c shows a magnified extract of the watershed segmentation result. The reader may consider that this are cuts through a 3-dimensional volume and lung segments. Observations of the results revealed some over and under-segmentations. Reasons for under-segmentation are weak demarcations between some high gray value areas in the rd-channel. Over-segmentation is apparently caused by inhomogeneous distribution of aerosol in the acini structures or imaging artifacts. To evaluate the rate of over- and undersegmentation a subset of manually annotated acini could be compared to the automated segmentation. This evaluation was not done jet as the observation of the results showed sufficient quality for further analysis and processing steps.

3.2.2 Sub-tree supply region segmentation

An alternative approach to split up the lung to smaller parts by not using the image information (rd channel) is to use the structure of the airway tree. This approach has the advantage that one can assign certain areas directly to parts of the airway tree. Lets take the second level of airway tree branches—so to speak every branch leaving the main airway in a lobe and call it a sub-tree. The space between these sub-trees can be divided and assigned to the nearest tree.

Subtree selection Which part of a airway-tree should be considered as sub-tree? This has to be individually decided by experts as some branches are difficult to assign in an automated fashion.

After labeling the sub-trees, one can see that the further away from

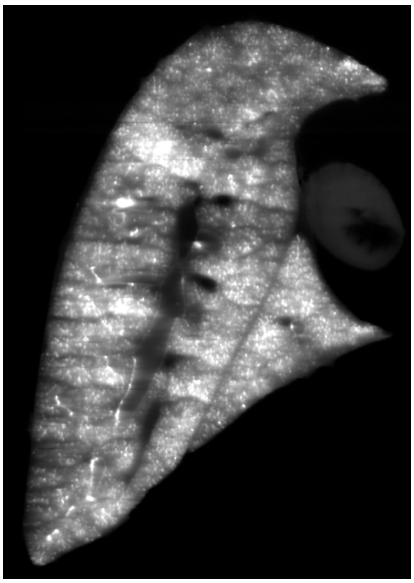

(a) Sagittal cut of the rd-channel

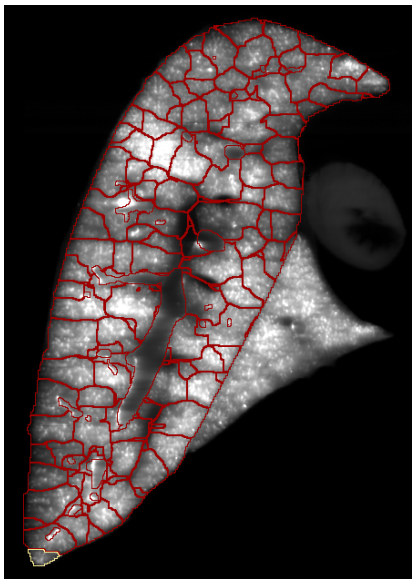

(b) Sagittal cut of rd-channel with acini partitions

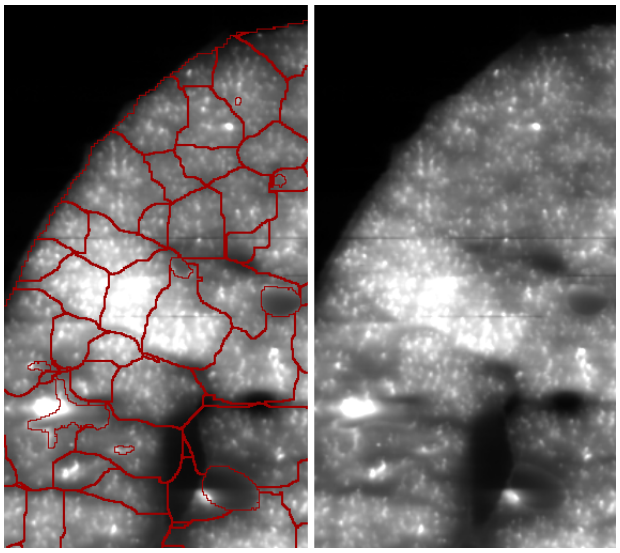

(c) Magnified region. Right: rd-channel, Left: Watershed segments borders over rd-channel

Figure 9: Acini partitions. Cross-section of a left lobe with segmented acini.

the root of the primary airway, the smaller the secondary branch gets, and therefore, the volume that such branches cover. Figure 10 shows an example of manually selected sub-trees of a rat lung.

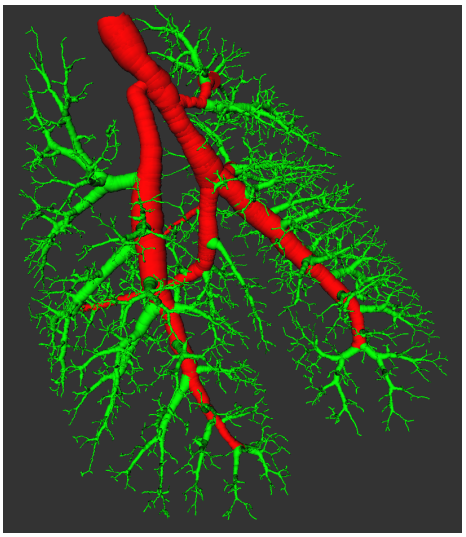

Figure 10: Airway Tree. An airwaytree with selected sub-trees (green). The main airway is depicted in red.

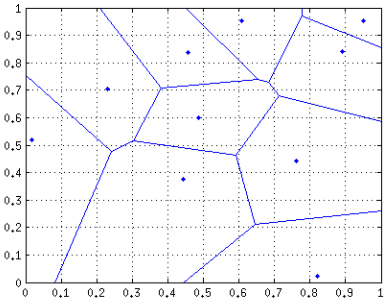

Figure 11: Voronoi Partitioning. A voronoi partitioned 2-dimensional area with 10 random seed points

Voronoi partitioning Voronoi partitioning is a simple way to estimate an area or volume based on seed points which also can be lines or areas. Every pixel respectively voxel in space gets assigned to the closest seed point. Figure 11 shows an example of a voronoi partitioned area.

This partitioning method was used to assign every voxel of a lobe volume to a sub-tree by using their center-lines as seed points. So every voxel got assigned to the sub-tree where the center-line is closest. The outcome of this method highly depends on the quality of the airway-tree segmentation. If a branch is not segmented, all voxel belonging to this airway would be assigned to a different branch and so distort measurements based on this partitioning.

Theoretically it's possible to recursively repeat this procedure to the generated sub-volumes and construct smaller sized partitions (i.e., selecting

sub-trees of the sub-trees and applying the voronoi-partitioner onto the sub-volumes). However, the resolution and quality of the provided volumes were not sufficient to produce such fine structured volumes.

Figure 13a shows the described voronoi-partitioning for a left lobe. Consider that the compartments are generated without the information of the rd-channel and thus represent just estimations and not segmentations of the supply region. That allows the borders to intersect areas which usually should be assigned to one sub-tree as a whole. One idea to improve the boundary and segment the supply regions according to anatomical structures is presented in the following section.

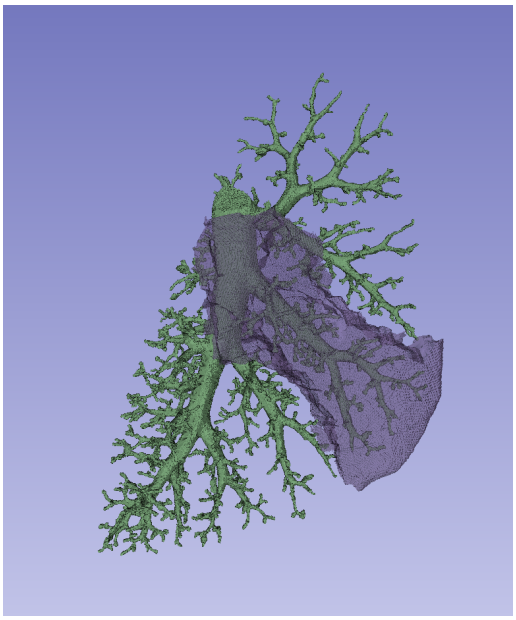

Figure 12: Supply Area. 3D visualization of a left-lobe's airways with half transparent estimated supply area and corresponding sub-tree.

Assigning acini segments to airway sub-trees As mentioned above, the estimated supply areas of the sub-trees have the big advantage, that the lung volume gets assigned to sub-trees and therefore allow inspection

and study correlations of airway-structure to perfusion and ventilation. However, the drawback is that in some cases, the boundaries don't follow anatomical structures. One possibility to overcome this issue is the combination of the compartments retrieved by watershed segmentation and the voronoi-partitions.

The method we used is quite straight forward. Every acinus segment got assigned to the sub-tree where most of its volume overlap to the sub-tree's voronoi-partition. So combined, the small compartments gather to sub-tree compartments with borders following the anatomical structures segmented by the watershed method and the approximate size of the estimated supply areas.

Results Figure 13b shows the consolidation of the smaller compartments to bigger sub-tree compartments. Figure 13d shows the differences and enhancements of the course of the borders by considering the acini compartments. Figure 13c allows to observe the borders of the combination approach. The reader can observe, that the compartment borders follow the anatomical structures. A more vivid visualization of a sub-tree compartment is given in Fig. 12.

3.2.3 Airway outlet supply region estimation

Another way of assigning the actual anatomical structures (acini compartments) to the airway tree, is to assign the compartments to the outlets of the airway sub-trees. That would theoretically allow to estimate the supply region of every airway outlet. However, due to the fact that the airway-tree can never be segmented perfectly, and therefore, will be lacking a number

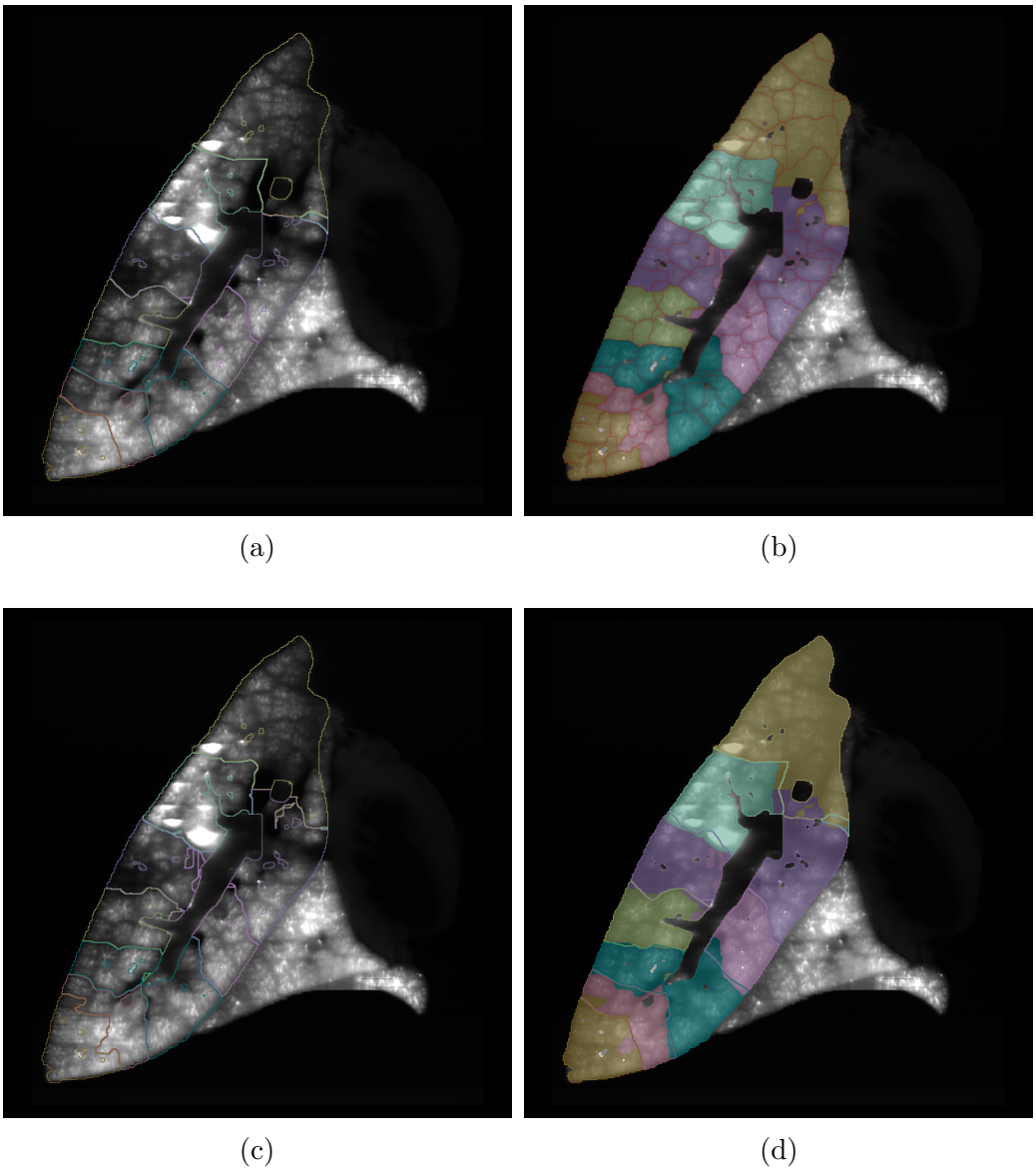

(a) (b)

(c) (d)

Figure 13: Improved sub-tree supply area calculation. Sagittal view of a left lobe with estimations of sub tree supply regions. The segmentation of the acini structures is used to improve the estimations of the sub-tree supply regions. (a) The Supply regions estimated by voronoi partitioning. (b) Acini partitions assigned to voronoi-partitions. (c) Outlines of the merged acini volumes. (d) Visualization of overlap between (a) and (c). The colored areas are the merged acini volumes. The lines indicate the borders of the voronoi-partitions.

of branches, some compartments will be assigned to an airway-end, which is actually not supplying this area. Also, the segmentation of the acini produced some over- and/or under-segmentation, thus there will be some wrong assignments to some airway-ends. Regardless of these problems, if data with higher resolution and sufficient airway-segmentation performance becomes available, this approach would allow to study the perfusion and ventilation of airway-outlet supplied regions. Two possible ways to assign acini to the airway outlets have been implemented.

Assignment by euler distance One idea was to calculate the center of mass of the acini compartments and assign them to the closest airway outlet. The airway outlets are extracted from the centerline representation of the airway segmentation. Each airway segment that doesn't represent the root and is without a connection to another segment is considered as an end-point.

Assignment by voronoi partition overlap This approach works similar to the method presented in Section 3.2.2. Voronoi partitions were made by using the airway outlets as seed points. The segments got assigned to the airway outlet having the biggest overlap with its vononoi partition.

Results Both methods showed similar results. Slight differences in the amount and size of calculated supply regions can be observed. For very good airway and acini segmentations, each acinus would be assigned to one airway outlet. Though, different inevitable shortcomings in the segmentation techniques have to be considered. For example, over segmentation of

the watershed method may cause the algorithm to merge small compartments to bigger ones, which are anatomically more accurate, but assuming that not all airway outlets are detected correctly, some independent regions may get merged erroneously.

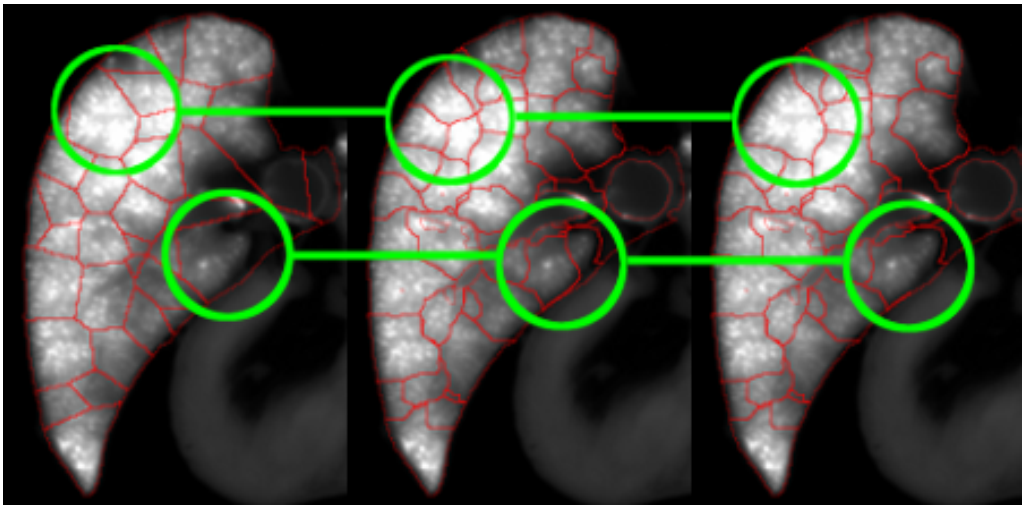

Figure 14: Airway outlets and their estimated supply region. At the very *left side* one can see the voronoi partitioning of a left lobe based on the airway outlets used as seed points. In the *middle*, the segmentation of the acini is shown, which are assigned to airway outlets at the *right side* of the figure. Cases where more than one acinus gets assigned to one airway outlet are highlighted with green markings.

4 Ventilation and Perfusion Data Analysis

An algorithm has been developed to calculate quantitative ventilation and perfusion data for the lung partitions generated by the methods described above. While perfusion data are represented by the sc-channel, information about ventilation is derived from the rd-channel. Dr. Glenny's laboratory provided the spatial locations of microspheres in the sc-channel for further processing.

Methods for counting the microspheres inside the compartments, summing up the gray values in the corresponding rd-channel, and measuring compartment sizes were developed. The voxel count allows to estimate the volume of the partitions, the sum of gray-value in the rd-channel provides knowledge regarding perfusion and the microsphere counts allow to draw conclusions on perfusion in the particular partition. The generated data was formatted/normalized for further processing and analysis as follows. For each volume i, the perfusion was calculated by

$$\dot{Q}_{i,meas} = \sum_{vol_i} (microspheres)/vol_i \ .$$

For the aerosol images (rd-channel), ventilation was estimated using

$$\dot{V}_{i,meas} = \sum_{vol_i} (grayscale - background)/vol_i \ .$$

The ventilation measurements need to be adjusted by subtraction of a background gray-value, because even in areas with no aerosol, the pixel gray-values are not zero. Without this correction, ventilation would be always overestimated. The background value was determined based on the cumulative histogram of the aerosol lung image by selecting the gray-value at the 5% level.

5 Results

It this work we have shown that it is possible to segment lung structures like lobes, secondary-lobes and even acini based on information gained from

different data channels of the imaging cryomicrotome. The average acini size of 7.9 μL corresponds well with measurements previously published in the literature. Also, the sub-structures of the lung generated with the presented methods were found to correlate well with expert tracings, but are less cumbersome to produce. The developed algorithms allow to study ventilation and perfusion in these partitions on different levels. For example, Fig. 15 depicts one example of perfusion and ventilation analysis for the computer generated compartments of a lobe. The presented methods enable

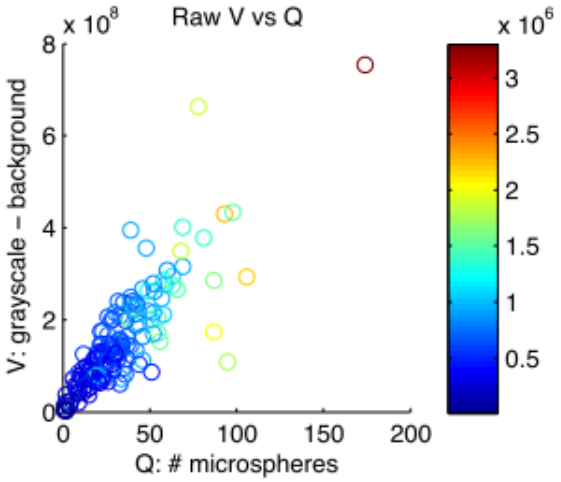

Figure 15: Correlation between perfusion and ventilation in a rat lung lobe based on identified lung compartments. The color represents the volume of compartments in voxel.

researchers to study the computer-identified lung structures in relation to corresponding airway and vessel geometry.

6 Conclusion

We presented algorithms to identify anatomical lung structures in cryomicrotome images of rat lungs on different levels. First, the rat lungs were partitioned into lobes based on user-selected points on fissures and by means of a surface interpolation approach. Second, structures on an acini level were segmented by utilizing a watershed segmentation approach. Third, sub-lobar regions were estimated based on airway sub-trees. To refine this estimation, identified acini compartments were assigned to sub-trees. In this context, two different algorithms were presented.

The generated partitions of the rat lung facilitate studies of local lung perfusion and ventilation, and allow to study regional lung function parameters in relation to geometric properties of corresponding airways and blood vessel. For this purpose, methods for calculating perfusion and ventilation in the identified lung partitions were implemented.

The developed methods are well suited to facilitate studies that analyse the influence of diseases on different lung regions and their functional indices.

References

[1] Jeffrey J. Kelly, Jon R. Ewen, Susan L. Bernard, Robb W. Glenny, and Clyde H. Barlow, "Regional blood flow measurements from fluorescent microsphere images using an imaging cryomicrotome," *Review of Scientific Instruments*, vol. 71, no. 1, pp. 228–234, 2000.